

---

# Selective Latent Thinking: Adaptive Compression of LLM Reasoning Chains

---

Hui Xie<sup>1</sup>, Jie Liu<sup>1\*</sup>, Ziyue Qiao<sup>2</sup>, Joaquin Vanschoren<sup>1</sup>

<sup>1</sup>Eindhoven University of Technology, Netherlands

<sup>2</sup>School of Computing and Information Technology, Great Bay University, China  
xiehui3019@gmail.com, {j.liu9, j.vanschoren}@tue.nl, zyxiao@gbu.edu.cn

## Abstract

Explicit chain-of-thought (CoT) reasoning substantially improves the reasoning ability of large language models (LLMs), but incurs high inference cost due to lengthy autoregressive traces. Existing latent reasoning methods offer a promising alternative, yet they often treat reasoning as uniformly compressible, causing precision-critical intermediate steps to be overly compressed and thereby degrading reasoning accuracy. In this work, we propose **Selective Latent Thinking (SLT)**, a framework that selectively compresses redundant reasoning spans into latent representations while preserving precision-critical spans as explicit CoT within the same reasoning trajectory. Specifically, SLT first uses a lightweight decoder to anticipate a short upcoming reasoning span, and then applies confidence-based gating to determine the longest span that can be reliably compressed. The accepted span is encoded into a compact latent representation to improve reasoning efficiency, while uncertain or precision-critical reasoning remains in explicit CoT form to preserve accuracy. To learn this selective compression policy, SLT adopts a three-stage training strategy that combines span-level latent compression, reliability-aware future reasoning prediction, and trajectory-level reinforcement learning to optimize the trade-off between answer correctness and reasoning cost. Extensive experiments across four mathematical reasoning benchmarks demonstrate that SLT achieves 22.7% higher accuracy than latent reasoning baselines at comparable compression ratios, while reducing reasoning chain length by 58.4% with only 2.8% accuracy degradation compared to explicit CoT. Our code can be found in <https://github.com/hunshi34/SLT>.

## 1 Introduction

As Large language models (LLMs) continue to scale, explicit chain-of-thought (CoT) reasoning [20, 22] has become a foundational paradigm for solving complex reasoning tasks. Recent advances further highlight its effectiveness when combined with reinforcement learning over long reasoning trajectories [9, 6, 18], yielding substantial improvements in reasoning capability. However, the inherent verbosity of CoT introduces high inference latency and substantial memory overhead, limiting efficiency and scalability [16, 4, 19].

Recent advances have sought to address this challenge by explicitly compressing CoT. One line of research operates at the token level, for example by identifying and skipping less informative tokens [21, 25, 7], encouraging models to produce more concise reasoning traces [23, 2, 1, 11], or terminating reasoning early once a sufficiently confident answer has been reached [24]. While effective, these methods remain confined to explicit token-level reasoning. A more promising alternative is to improve efficiency by performing reasoning process within dense latent spaces. Pioneering works

---

\*Corresponding author

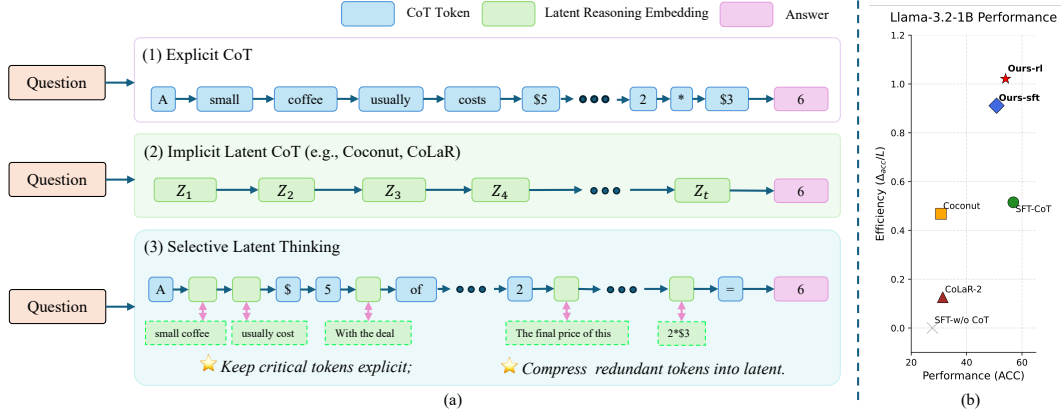


Figure 1: **Comparison of reasoning paradigms and efficiency analysis.** (a) Explicit CoT relies on verbose textual generation, whereas implicit latent CoT compresses the reasoning into latent space. Our **Selective Latent Thinking** (SLT) instead dynamically interleaves explicit CoT and latent reasoning, preserving precision-critical tokens in explicit form while selectively compressing redundant reasoning into latent. (b) SLT achieves a superior accuracy–efficiency trade-off ( $\Delta_{acc}/L$ ) compared with both explicit CoT and implicit latent reasoning baselines.

such as Coconut [8] and CODI [15] laid the foundation for latent reasoning by distilling explicit CoT into continuous latent representations. More recent methods, such as CoLaR [17] and RoT [19], further extend this paradigm through dynamic latent compression and alternative latent reasoning forms. However, these methods typically adopt a **homogeneous compressibility assumption**, where intermediate reasoning spans are regarded as uniformly suitable for latent compression. This assumption does not always hold in precision-sensitive settings such as mathematical reasoning, where certain critical reasoning spans often need to remain explicit in order to preserve correctness.

To address these challenges, we introduce **Selective Latent Thinking (SLT)**, a framework that *selectively compresses redundant reasoning spans into latent representations while preserving precision-critical intermediate reasoning spans in explicit CoT form* (Figure 1 (a)). Specifically, SLT introduces a dynamic switching mechanism built upon three components: a backbone LLM, a reliability-aware feature decoder, and a latent compressor. Instead of compressing reasoning uniformly, SLT first uses the feature decoder to anticipate upcoming reasoning spans. A confidence gate then identifies the longest reliable span that can be safely compressed. The accepted span is encoded into a compact latent representation, allowing the model to bypass multiple autoregressive reasoning steps. When the predicted trajectory is uncertain, such as around precision-critical mathematical operations, SLT automatically falls back to explicit CoT. To learn this selective behavior, we introduce a three-stage training strategy. First, we train the latent compressor to encode explicit reasoning spans into compact latent representations. Second, we jointly optimize future trajectory prediction and confidence estimation, enabling the model to anticipate upcoming reasoning and assess whether compression is trustworthy. Third, we apply trajectory-level reinforcement learning to optimize the global trade-off between answer correctness and explicit reasoning cost. This allows SLT to learn a dynamic reasoning policy that balances reasoning efficiency and logical fidelity by selectively interleaving latent reasoning with explicit CoT.

We comprehensively evaluate SLT on a suite of mathematical reasoning benchmarks, from standard datasets (e.g., GSM8k-AugNL, SVAMP) to the highly challenging MATH500. Empirical results on the Llama-3.2-1B and Qwen3-4B backbones demonstrate that SLT establishes a superior trade-off between accuracy and efficiency. As shown in Figure 1 (b), SLT significantly outperforms state-of-the-art latent reasoning baselines while drastically reducing the token footprint of explicit CoT. In summary, our contributions are:

- We propose Selective Latent Thinking (SLT), a novel framework that enables dynamic switching between latent thinking and explicit CoT within a single reasoning trajectory.
- We introduce a reliability-aware feature decoding mechanism with confidence gating that enables selective latent compression by identifying compressible reasoning spans while preserving precision-critical intermediate reasoning steps in explicit form.

- Extensive experiments across multiple benchmarks and model scales demonstrate that SLT achieves a superior trade-off between reasoning accuracy and length of reasoning chain, consistently outperforming state-of-the-art latent reasoning baselines.

## 2 Related Work

**Efficient Reasoning with Explicit CoT Reduction.** A related line of work improves reasoning efficiency by reducing the cost of explicit Chain-of-Thought (CoT) generation. Some methods operate at the token level, for example by skipping less informative tokens or encouraging shorter reasoning traces [21, 23, 2, 1, 11]. Others reduce unnecessary reasoning at the trajectory level through adaptive stopping or budget allocation [24, 16, 4]. While effective, these approaches remain within the explicit token space and primarily aim to shorten reasoning trajectories. In contrast, our method reduces reasoning cost by selectively replacing compressible reasoning spans with latent representations, while preserving explicit CoT for precision-critical computation.

**Latent Reasoning and Continuous Thought.** Complementary to explicit CoT reduction, another line of work improves reasoning efficiency by shifting the reasoning process into continuous latent representations. Early methods such as Coconut [8] and CoDi [15] establish this paradigm by distilling explicit CoT segments into latent tokens. Subsequent work further develops this idea: Compressed CoT [14] represents implicit reasoning as dense latent sequences, while CoLaR [17] improves latent decodability through additional structural constraints. More recent approaches, including RoT [19] and OneLatent [12], broaden latent reasoning to multimodal settings by coupling LLM hidden states with visual features. Unlike these methods, which predominantly reason directly in latent space, our framework first anticipates a short explicit reasoning trajectory and then selectively compresses only the accepted span into a compact latent representation.

**Multi-Token Prediction and Future Anticipation.** Recent advances improve autoregressive decoding efficiency by predicting multiple future tokens or intermediate representations in parallel. Representative examples include Medusa [3], which augments the backbone model with multiple decoding heads, as well as multi-token prediction methods such as Better & Faster Large Language Models via Multi-token Prediction [5] and Your LLM Knows the Future [13], which leverage the model’s ability to anticipate several upcoming tokens from a shared prefix. At the feature level, EAGLE-3 [10] further demonstrates that predicting future representations can substantially reduce decoding latency. Collectively, these works show that future tokens and intermediate representations can be reliably anticipated from the current context. We build on this insight by using a lightweight feature decoder to roll out short candidate reasoning trajectories, which serve as the basis for deciding where latent compression is appropriate.

## 3 Method

### 3.1 Overview

In this section, we introduce **Selective Latent Thinking (SLT)**, a framework that dynamically interleaves latent reasoning and explicit CoT within a single reasoning trajectory. The key idea is to replace only those intermediate reasoning spans that can be reliably compressed into latent representations, while preserving explicit reasoning form for the remaining steps. As shown in Figure 2, SLT consists of three components: a primary large language model (LLM), a lightweight feature decoder  $\mathcal{D}$ , and a latent compressor  $\mathcal{C}$ .

During reasoning, the primary LLM maintains the current autoregressive state. Conditioned on the current hidden states of the primary LLM, the feature decoder  $\mathcal{D}$  predicts a short future reasoning trajectory  $x_{1:j}^{\mathcal{D}}$  that approximates the next few explicit CoT steps. A confidence gating module then evaluates this predicted trajectory and selects the longest continuous prefix that is reliable enough for latent compression. Formally, let  $\mathbf{h}_j^{\mathcal{D}}$  denote the hidden state of  $\mathcal{D}$  at step  $j$ . The gate projects this hidden state to a scalar confidence logit:

$$c_j = \mathbf{w}_{\text{gate}}^\top \mathbf{h}_j^{\mathcal{D}} + b_{\text{gate}}, \tag{1}$$

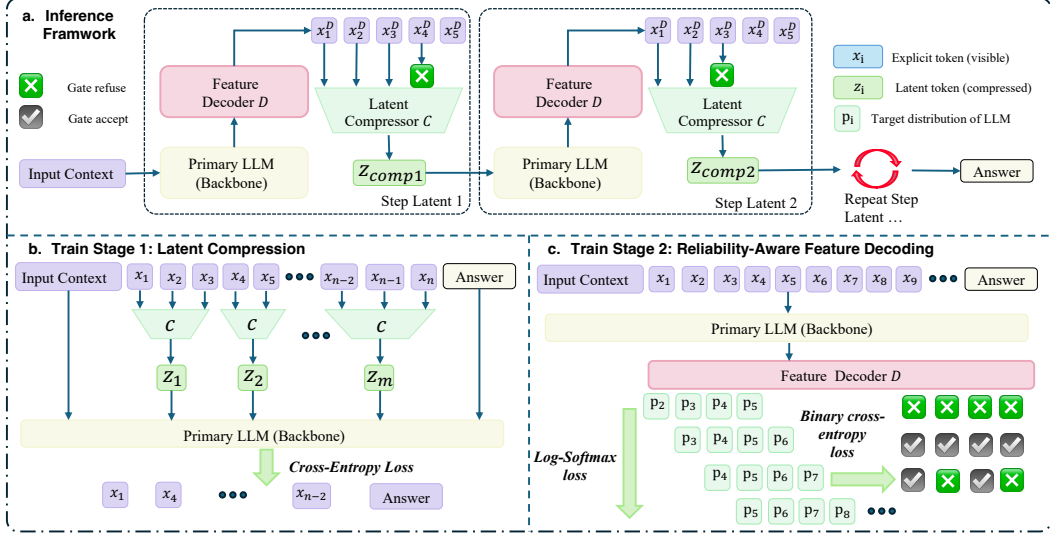


Figure 2: **Overview of the proposed Selective Latent Thinking (SLT).** (a) During inference, a lightweight decoder  $\mathcal{D}$  predicts a short future reasoning trajectory, a confidence gate selects the reliable prefix, and the latent compressor  $\mathcal{C}$  maps the accepted span into a single latent block for efficient LLM state updates. (b) The compressor is trained to replace multi-step reasoning spans with latent blocks while preserving causal alignment. (c) The decoder and gate are jointly trained to predict future reasoning and determine which spans are reliable enough for latent compression.

and accepts the longest prefix of length  $n \leq K$  such that  $c_i > \tau$  for all  $i \leq n$ , where  $\tau$  is a predefined threshold. The accepted span is then encoded by the latent compressor  $\mathcal{C}$  into a fixed-length latent:

$$\mathbf{z}_{\text{comp}} \in \mathbb{R}^{1 \times d}. \quad (2)$$

This latent block is injected back into the primary LLM as a proxy embedding for the next autoregressive update, allowing multiple explicit reasoning steps to be replaced by a single latent transition. If no sufficiently reliable prefix is found, SLT simply continues with standard explicit CoT generation.

Once the model reaches the `</think>` token, the system exits the latent reasoning mode and reverts to standard autoregressive decoding. In this final answer generation phase, both  $\mathcal{D}$  and  $\mathcal{C}$  are disabled, so that the user-facing response is produced directly by the original LLM.

### 3.2 Latent Compression Learning

We first train the latent compressor  $\mathcal{C}$  to encode explicit reasoning spans into compact latent representations that can be integrated into the autoregressive computation of the primary LLM. The goal of this stage is to establish the model’s ability to replace multi-step explicit reasoning with a single latent transition while preserving causal consistency.

We implement  $\mathcal{C}$  as a cross-attention bottleneck. To preserve the sequential structure of the compressed span, we add learnable positional encodings to the token embeddings before compression. A learnable latent query then attends to these position-aware contextualized embeddings, producing a fixed-length latent representation. Given a reasoning span  $\mathbf{x}_{t:t+N-1}$  of length  $N$ , the compressor outputs

$$\mathbf{z}_{\text{comp}} = \mathcal{C}(\mathbf{x}_{t:t+N-1}) \in \mathbb{R}^{1 \times d}. \quad (3)$$

In practice, this bottleneck is effective at compressing smooth logical transitions, but less effective at preserving high-entropy discrete entities such as exact mathematical values. We empirically verify this limitation in Section 4.3. Accordingly, this stage is designed to learn *how* to compress reasoning spans, while the decision of *when* latent compression should be applied is deferred to the reliability-aware mechanism introduced in the next stage.

**Hybrid Sequence and Causal Alignment.** To integrate latent representations into autoregressive decoding, we construct a hybrid sequence  $\mathcal{S}_{\text{hybrid}}$  by replacing each contiguous reasoning span with

a latent block of length 1, whose embedding is given by  $\mathbf{z}_{\text{comp}}$ . We then enforce causal alignment between the original sequence and the hybrid sequence. Specifically, if the compressed span begins at token  $x_t$  and ends at  $x_{t+N-1}$ , the prefix state immediately before the latent block is trained to predict  $x_t$ , and the latent position is trained to predict  $x_{t+N}$ , i.e., the first token following the removed span.

We optimize the standard language modeling objective on the aligned hybrid sequence:

$$\mathcal{L}_{\text{comp}} = - \sum_j \log P(y_j \mid \mathcal{S}_{\text{hybrid}, <j}), \quad (4)$$

where the targets  $y_j$  follow the alignment rule above. This objective encourages the latent block to preserve the information necessary to bridge the compressed span and predict the continuation.

### 3.3 Reliability-Aware Feature Decoding

Latent compression learning equips the model with the ability to compress explicit reasoning spans into latent representations, but does not determine when latent compression is appropriate. Prior latent reasoning methods often rely on a **homogeneous compressibility assumption**, implicitly treating different parts of a reasoning trajectory as equally suitable for latent compression. In practice, however, the predictability of future reasoning varies substantially across spans, especially in precision-sensitive settings. To address this, we train a lightweight feature decoder with a confidence gate to estimate which predicted reasoning steps are reliable enough for latent compression.

Given the current hidden state of the primary LLM, the feature decoder  $\mathcal{D}$  predicts a short future reasoning trajectory. Let  $\mathbf{p}_j^{\mathcal{D}}$  denote the output distribution of  $\mathcal{D}$  at step  $j$ , and let  $\mathbf{p}_j^{\text{LLM}}$  denote the corresponding target distribution from the primary LLM. We train  $\mathcal{D}$  by matching these distributions:

$$\mathcal{L}_{\text{vocab}} = - \sum_j \sum_{v \in \mathcal{V}} p_{j,v}^{\text{LLM}} \log p_{j,v}^{\mathcal{D}}. \quad (5)$$

To supervise the gate, we define a relaxed binary continuation label based on mutual top- $k$  inclusion:

$$y_j^{\text{gate}} = \mathbb{I} [\hat{x}_j^{\mathcal{D}} \in \mathcal{T}_3(\mathbf{p}_j^{\text{LLM}}) \wedge \hat{x}_j^{\text{LLM}} \in \mathcal{T}_3(\mathbf{p}_j^{\mathcal{D}})], \quad (6)$$

where  $\hat{x}$  denotes the top-1 predicted token, and  $\mathcal{T}_3(\mathbf{p})$  denotes the set of top-3 token indices from distribution  $\mathbf{p}$ . This relaxed criterion avoids penalizing predictions that differ at the top-1 token but remain highly consistent at the distribution level.

The gating module outputs a raw confidence logit  $c_j$ , which is optimized using a weighted binary cross-entropy with logits loss:

$$\mathcal{L}_{\text{gate}} = - \sum_j w_j (y_j^{\text{gate}} \log \sigma(c_j) + (1 - y_j^{\text{gate}}) \log(1 - \sigma(c_j))), \quad (7)$$

where  $\sigma$  is the sigmoid function used only for loss computation. The overall objective for this stage is

$$\mathcal{L}_{\text{decode}} = \mathcal{L}_{\text{vocab}} + \lambda \mathcal{L}_{\text{gate}}. \quad (8)$$

Jointly training future trajectory prediction and confidence estimation allows the model to assess the correctness of the predicted future reasoning at each local step. As a result, the feature decoder learns not only to anticipate future reasoning, but also to produce representations that are informative for compression reliability estimation.

A practical complication is that the explicit LLM distribution for the continuous `<compress>` token is undefined, making direct token-level supervision for latent steps infeasible. To better align the gate with actual inference-time behavior, we therefore include an additional verification phase on a 50k-sample subset. In this phase, the frozen primary LLM evaluates the feature decoder’s predictions and provides binary acceptance labels, which are used to further refine the gating module. This step helps bridge the gap between discrete training-time supervision and the model’s actual acceptance of continuous latent representations during inference.

### 3.4 Trajectory-Level Accuracy–Cost Optimization

The first two stages establish local mechanisms for latent compression and reliability estimation, but they do not directly optimize the long-horizon consequences of compression decisions. A locally acceptable latent substitution may still harm the final answer if its errors propagate through the remaining reasoning trajectory. To address this long-horizon credit assignment problem, we formulate the full **Selective Latent Thinking (SLT)** framework as a sequential decision process and optimize the joint policy  $\pi_\theta(\tau | x)$  using Group Relative Policy Optimization (GRPO).

To balance reasoning accuracy against explicit reasoning cost. To this end, we define a delayed reward that favors correct final answers while penalizing unnecessary explicit token generation:

$$r(\tau) = \mathbb{I}[\text{Correct}(\tau)] \cdot (\alpha - \beta \cdot T_{\text{LLM}}(\tau)), \quad (9)$$

where  $\mathbb{I}[\text{Correct}(\tau)] \in \{0, 1\}$  indicates whether the final answer is correct, and  $T_{\text{LLM}}(\tau)$  denotes the total number of CoT tokens generated by the primary LLM along trajectory  $\tau$ . In our implementation, we omit the conventional KL-divergence penalty against a reference model to reduce training overhead, as the deterministic reward intrinsically prevents reward hacking. The optimization objective is:

$$\mathcal{J}_{\text{RL}}(\theta) = \mathbb{E}_{\tau \sim \pi_\theta}[r(\tau)]. \quad (10)$$

Trajectory-level optimization allows the policy to account for the delayed effects of local decisions. Thus, the model learns when latent compression improves efficiency without harming correctness, and when explicit CoT should be preserved to maintain performance on precision-critical steps.

## 4 Experiments

### 4.1 Experiment Settings

**Datasets and Tasks.** We primarily train and evaluate our framework on **GSM8k-AugNL**, which contains roughly 385k training instances and over 1k test instances. We use this as our main setting because it better reflects the free-form natural-language CoT style commonly used in practice. To evaluate robustness, we additionally test on **GSM-Hard**, **SVAMP**, and **MultiArith**. We also report results on the original **GSM8k-Aug** dataset, whose more structured rationale format (e.g., tagged intermediate spans like “ $\llbracket 5 \cdot 2 = 10 \rrbracket \llbracket 30 / 10 = 3 \rrbracket$ ”) is better matched to prior latent reasoning baselines such as **CoLaR-2** and **Coconut**. Finally, we study cross-domain transfer on **Math500**, using an additional math-domain training set with 7.5k training instances and 0.5k test instances.

**Baseline Methods.** We compare against several standard and state-of-the-art baselines. **SFT-w/o CoT** is trained by discarding reasoning steps from the dataset, forcing the model to output the final answer directly ( $L = 0$ ). **SFT-CoT** is the standard full-parameter fine-tuning baseline trained with complete CoT rationales. For efficient and latent reasoning baselines, we compare against **Coconut**, **CoLaR-2**, and **RoT**. We evaluate our framework in two settings: **Ours-SFT**, corresponding to the model after Sec. 3.3 training, and **Ours-RL**, corresponding to the final model after reinforcement learning. All reported lengths (#L) represent explicit CoT tokens only. As a coarse proxy for the accuracy–efficiency trade-off, we also report  $\Delta_{\text{acc}}/L$ , defined as the accuracy improvement over **SFT-w/o CoT** divided by CoT length.

**Implementation Details.** We employ Llama-3.2-1B and Qwen3-4B as our primary backbones. To establish strong reasoning baselines, both models are first fully fine-tuned on GSM8k-AugNL. For our framework, Stage 1 trains the latent compressor with LoRA using a progressive schedule that gradually increases the proportion of compressed CoT spans. Stage 2 freezes the primary LLM and trains the feature decoder and confidence gate. Stage 3 unfreezes all modules and performs joint optimization with reinforcement learning. For fair comparison, we applied greedy decoding to all evaluated methods if applicable. Full hyperparameter settings are provided in the Appendix.

### 4.2 Main Results

**Comparison to baseline methods on GSM datasets.** Table 1 compares SLT with state-of-the-art baselines on four grade-school mathematical reasoning benchmarks. SLT consistently achieves a stronger accuracy–efficiency trade-off than prior latent reasoning methods. In particular, on Llama-3.2-1B, **Ours-RL** improves average accuracy by 23.04% relative to CoLaR-2 while using fewer CoT

Table 1: Performance and sequence length comparison across multiple reasoning benchmarks. Results marked with † are reported from the RoT baseline paper, while all Llama-3.2-1B results, as well as the SFT-w/o CoT and our models on Qwen3-4B, are based on our local evaluations. **Pass@1** denotes the accuracy of the first generated response (%). **# L** represents the average number of generated reasoning or latent tokens.  $\Delta_{acc}/L$  measures the reasoning efficiency, defined as the average accuracy improvement over the SFT-w/o CoT baseline divided by the average reasoning length.

	GSM		GSM-Hard		SVAMP		MultiArith		Average		
	Pass@1	# L	Pass@1	# L	Pass@1	# L	Pass@1	# L	Pass@1	# L	$\Delta_{acc}/L$
<i>Llama-3.2-1B</i>											
SFT-w/o CoT	21.23	0.00	5.00	0.00	43.70	0.00	41.67	0.00	27.65	0.00	-
SFT-CoT	53.49	77.89	13.40	89.25	63.40	39.18	97.20	42.20	56.87	62.13	0.515
Coconut	24.24	6.00	5.49	6.00	40.70	6.00	52.55	6.00	30.74	6.00	0.468
CoLaR-2	17.23	37.85	3.86	42.00	34.40	20.21	70.18	19.33	31.40	29.84	0.126
<b>Ours-SFT</b>	40.76	31.25	10.91	42.07	59.40	14.21	92.22	14.16	50.82	25.42	0.911
<b>Ours-RL</b>	<b>46.47</b>	32.09	<b>11.52</b>	43.35	<b>61.60</b>	13.88	<b>96.67</b>	14.18	<b>54.07</b>	25.87	<b>1.021</b>
<i>Qwen3-4B</i>											
SFT-w/o CoT	38.44	0.00	14.18	0.00	72.90	0.00	93.33	0.00	54.71	0.00	-
SFT-CoT	82.18	85.20	50.23	117.30	84.20	36.80	100.00	40.90	79.15	70.05	0.348
Coconut†	16.90	6.00	5.42	6.00	43.60	6.00	60.30	6.00	31.60	6.00	-3.852
CoLaR-2†	40.00	39.60	9.17	47.40	57.70	19.20	82.20	21.10	47.30	31.80	-0.233
RoT†	37.80	32.00	14.10	32.00	72.70	32.00	97.20	32.00	55.40	32.00	0.022
<b>Ours-SFT</b>	63.84	38.84	29.72	64.49	76.20	15.90	95.00	17.69	66.19	34.23	0.335
<b>Ours-RL</b>	<b>75.28</b>	38.36	<b>35.10</b>	63.90	<b>81.10</b>	14.75	<b>99.44</b>	15.70	<b>72.73</b>	33.17	<b>0.543</b>

Table 2: Additional comparison on the original GSM8k-Aug rationale format. Methods marked with a dagger (†) are cited from CoLaR’s original paper, while all other results are obtained through our local implementation and evaluation. This table evaluates models on a format compatible with several prior latent reasoning baselines. Each benchmark reports Pass@1 and CoT length (#L) separately.

Method	GSM		GSM-Hard		SVAMP		MultiArith		Average	
	Pass@1	#L	Pass@1	#L	Pass@1	#L	Pass@1	#L	Pass@1	#L
SFT-CoT	52.77	25.20	13.04	34.60	64.90	11.30	97.22	14.30	56.98	21.35
Coconut†	23.10	6.00	5.49	6.00	40.70	6.00	41.10	6.00	27.59	6.00
CoLaR-2†	40.10	12.70	9.08	14.00	54.90	6.11	91.30	7.35	48.84	10.04
<b>Ours-SFT</b>	42.46	13.42	9.33	22.35	58.30	6.43	95.00	5.73	51.27	11.98
<b>Ours-RL</b>	<b>47.23</b>	13.23	<b>10.77</b>	21.03	<b>60.80</b>	<b>5.86</b>	<b>98.89</b>	<b>5.68</b>	<b>54.42</b>	11.45

tokens (25.87 vs. 29.84). Relative to explicit CoT, it reduces reasoning length by 58.4% with only 2.8% performance degradation. This advantage stems from SLT’s ability to preserve explicit reasoning for precision-critical spans and compress redundant reasoning steps into latent representations, rather than compressing the reasoning trajectory uniformly into latent form. On Qwen3-4B, **Ours-RL** improves average accuracy over RoT by 17.33% at a comparable compression ratio, indicating that selective fallback to explicit CoT remains beneficial for precision-sensitive reasoning with stronger models. Furthermore, the consistent improvement of **Ours-RL** over **Ours-SFT**, e.g., 54.07% vs. 50.82% on Llama-3.2-1B, demonstrates that trajectory-level reinforcement learning effectively turns locally trained compression and gating modules into a coherent selective compression policy. Since the FLOP overhead of our auxiliary modules is negligible compared to the LLM backbone, this token reduction yields an actual wall-clock speedup (see Appendix A).

**Results on the Original GSM8k-Aug Format.** Table 2 presents results on the original GSM8k-Aug rationale format, which contains more structured and equation-oriented reasoning than GSM8k-AugNL. This setting provides a controlled comparison with prior latent reasoning baselines such as Coconut and CoLaR-2, while evaluating whether SLT can compress mathematical reasoning beyond merely removing linguistic redundancy. Even under this more structured format, SLT consistently outperforms latent reasoning baselines, surpassing CoLaR-2 by 5.58% in average accuracy with comparable CoT length. Relative to explicit CoT, SLT incurs only a 2.56% accuracy drop while reducing reasoning length by 46.27%. This advantage is especially clear on MultiArith, where **Ours-RL** outperforms SFT-CoT (98.89% vs. 97.22%) while reducing CoT length from 14.30 to 5.68. These results highlight that SLT improves efficiency by selectively compressing mathematical reasoning itself, rather than simply reducing redundancy in free-form CoT.

Table 3: Results on Math500. SFT-w/o CoT, SFT-CoT, and Ours-SFT (math) are trained on math-domain data and evaluated on Math500. Ours-RL (gsm) and Ours-SFT (gsm) are the models trained on GSM8k-AugNL from Table 1, directly evaluated on Math500.

Backbone	SFT-w/o CoT		SFT-CoT		Ours-SFT (math)		Ours-SFT (gsm)		Ours-RL (gsm)	
	Acc	#L	Acc	#L	Acc	#L	Acc	#L	Acc	#L
Llama-3.1-1B	8.22	0.00	14.00	205.83	11.60	112.32	10.80	97.80	14.60	90.02
Qwen3-4B	29.40	0.00	53.20	248.20	34.40	100.03	41.20	132.29	42.60	107.77

Table 4: Isolated evaluation of the Latent Compressor (Stage 1). “Ratio” indicates the retained CoT length relative to the full SFT-CoT.  $\dagger$  denotes the specific retention ratio on the GSM-Hard dataset. *Compress-Random* blindly compresses every 2–5 tokens, while *Compress-SkipNum* explicitly preserves numeric tokens, highlighting the importance of retaining critical mathematical values.

Method	Llama-3.2-1B				Qwen3-4B			
	Ratio	SVAMP	MultiArith	GSM-Hard	Ratio	SVAMP	MultiArith	GSM-Hard
SFT-CoT	100%	63.40	97.20	13.40	100%	85.50	100.00	54.70
Compress-Random	~30%	60.50	98.30	10.90	~30%	78.00	95.60	17.29
Compress-SkipNum	~50% (60% $\dagger$ )	<b>63.40</b>	<b>97.78</b>	<b>13.30</b>	~57% (80% $\dagger$ )	<b>84.60</b>	<b>100.00</b>	<b>51.80</b>

**Out-of-domain Generalization to Math500.** Table 3 presents out-of-domain generalization results on the more challenging Math500. The results show that **Ours-RL (gsm)** finetuned on GSM-AugNL dataset generalizes competitively despite never being trained on Math500-style data. On Llama-3.1-1B, it slightly outperforms the in-domain **SFT-CoT** baseline (14.60 vs. 14.00) while reducing reasoning length by 56.3% (90.02 vs. 205.83). On Qwen3-4B, it remains below in-domain **SFT-CoT** but substantially improves over **Ours-SFT (gsm)** (42.60 vs. 41.20) with shorter reasoning length (107.77 vs. 132.29), indicating that trajectory-level RL improves transfer of the selective compression policy. When trained directly on the math-domain data, **Ours-SFT (math)** also achieves a favorable accuracy–efficiency trade-off. On Llama-3.1-1B, it incurs only a 2.40% accuracy drop compared with **SFT-CoT** (11.60 vs. 14.00), while reducing reasoning length by 45.4% (112.32 vs. 205.83). These results show that SLT can substantially reduce reasoning cost both under cross-domain transfer and in-domain training, while retaining competitive mathematical reasoning performance.

### 4.3 Ablation Study & Analysis

**Effects of Selective Compression.** To investigate the effectiveness of selective compression, we compare two heuristic compression strategies using the same trained latent compressor. *Compress-Random* represents a non-selective baseline that compresses randomly sized token chunks ( $c \sim U(2, 5)$ ) into single latent embeddings. *Compress-SkipNum* represents a simple selective strategy that preserves numeric tokens and compresses only the surrounding text. Together with SFT-CoT, these comparisons allow us to test whether reasoning spans can be compressed uniformly, or whether precision-critical spans need to remain explicit. As shown in Table 4, *Compress-Random* substantially reduces CoT length but severely degrades accuracy on precision-sensitive tasks, especially GSM-Hard. In contrast, *Compress-SkipNum* recovers most of the lost performance while still maintaining a compact trajectory. This contrast shows that reasoning spans are not uniformly compressible, motivating SLT’s reliability-aware gating mechanism to learn such compression decisions adaptively. Examples in Figure 3 further demonstrates that SLT effectively compresses linguistic context while preserving precision-critical numerical and arithmetic steps.

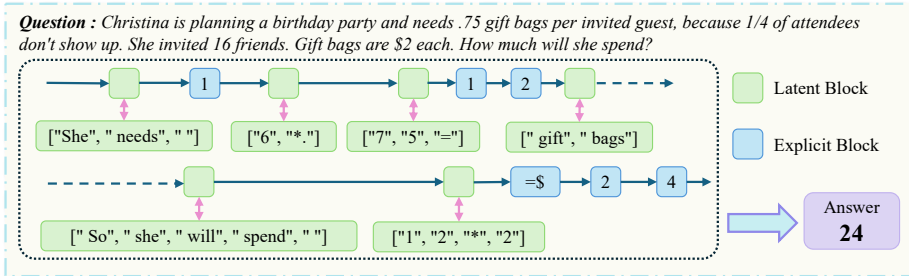


Figure 3: **Example of SLT reasoning trajectories.** SLT dynamically interleaves latent transitions with explicit reasoning while preserving precision-critical numerical and arithmetic steps.

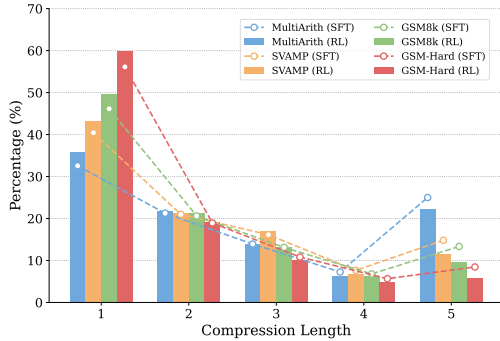


Figure 4: **Compression length distribution.** Bars show the RL policy, while dashed lines show the supervised policy before RL. SLT adaptively uses shorter or longer compression lengths depending on dataset difficulty.

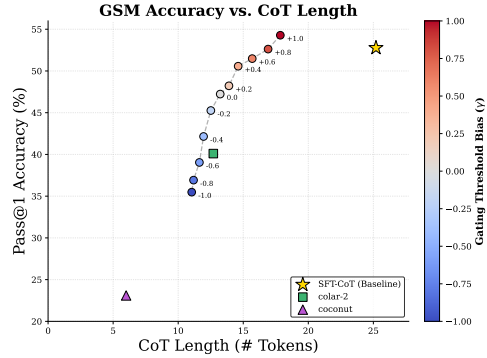


Figure 5: **Gating threshold and performance analysis on GSM.** Varying the gating threshold produces a smooth accuracy–efficiency frontier, showing that SLT can control CoT length while approaching full CoT accuracy.

### Effects of Confidence Gating Strategy.

Table 5 evaluates the role of the confidence gate in deciding whether predicted reasoning spans should be compressed. Removing the gate entirely (*w/o Gate*) leads to a severe performance drop, e.g., from 29.72 to 1.67 on GSM-Hard, showing that latent predictions cannot be accepted indiscriminately. Training the gate without joint optimization with the feature decoder (*w/o Joint Gate*) also consistently degrades performance compared with *Ours-SFT*. These results indicate that confidence gating is essential for reliable latent compression, and that joint training is necessary to align future trajectory prediction with compression reliability estimation.

Table 5: Ablation on Stage 2 joint gate training comparing three settings: (1) Ours-SFT: our complete joint training and refinement strategy; (2) w/o Joint Gate: isolated post-hoc refinement only; (3) w/o Gate: no confidence gating.

Training Strategy	SVAMP	MultiArith	GSM	GSM-Hard
Ours-SFT	76.20	95.00	63.84	29.72
w/o Joint Gate	72.40	93.89	57.77	27.90
w/o Gate	24.60	15.00	6.37	1.67

### Effects of Gating Threshold.

Figure 5 analyzes how the gating threshold modulates the trade-off between accuracy and CoT length. Lower thresholds accept longer predicted spans for latent compression, leading to shorter explicit reasoning trajectories, whereas higher thresholds impose stricter reliability requirements and preserve more explicit CoT. Across thresholds, SLT traces a smooth Pareto frontier: accuracy improves steadily as more explicit reasoning is retained. This indicates that the confidence gate provides a controllable mechanism for navigating the accuracy–efficiency trade-off rather than producing a single fixed operating point. Compared with prior latent reasoning baselines, SLT achieves higher accuracy at comparable CoT lengths, and approaches the performance of full SFT-CoT while requiring substantially shorter reasoning trajectories.

### Compression Policy Analysis.

Figure 4 visualizes the accepted compression lengths ( $c = 1$  to 5). Overall, the policy generally favors shorter spans, gradually decreasing from  $c = 1$  to 4, which reflects the frequent need to halt compression before unpredictable, precision-critical mathematical steps. The notable accumulation at  $c = 5$  is simply an artifact of capping safely compressible longer spans at the maximum look-ahead window. Comparing the policies, RL shifts the distribution towards a more conservative and robust regime: cautious short compressions ( $c = 1$ ) increase, while maximum-length compressions ( $c = 5$ ) decrease. Crucially, although RL favors shorter latent transitions, the overall explicit CoT length does not increase (Table 1). By proactively penalizing unreliable long compressions, RL prevents the severe state corruption and rambling recovery trajectories that typically follow, ultimately achieving a more compact and accurate reasoning chain.

## 5 Conclusion and Limitations

We introduced **Selective Latent Thinking (SLT)**, a dynamic framework that interleaves latent thinking and explicit CoT within a single reasoning trajectory. By anticipating short future reasoning spans,

estimating their reliability through confidence-based gating, and selectively compressing accepted spans, SLT preserves precision-critical steps in explicit form. Trajectory-level reinforcement learning further optimizes this switching policy to maximize both accuracy and efficiency. Experiments across multiple mathematical reasoning benchmarks demonstrate that SLT achieves a superior accuracy–efficiency trade-off compared to prior latent reasoning baselines. Ultimately, our findings highlight the necessity of moving beyond uniform compression to explicitly model the selective compressibility of intermediate reasoning.

Despite these promising results, our current study is limited in terms of model scale and reasoning length. Due to the high computational cost of training the feature decoder, latent compressor, and trajectory-level RL policy, our evaluations are primarily restricted to the Llama-3.2-1B and Qwen3-4B backbones. We have not yet extended this framework to long-form thinking models that generate substantially longer reasoning traces. In future work, we plan to address these constraints by exploring more computationally efficient training and RL optimization strategies. This will enable us to scale SLT to further validate its efficacy on highly extended reasoning trajectories.

## References

- [1] Pranjal Aggarwal and Sean Welleck. L1: Controlling how long a reasoning model thinks with reinforcement learning. *arXiv preprint arXiv:2503.04697*, 2025.
- [2] Simon A Aytes, Jinheon Baek, and Sung Ju Hwang. Sketch-of-thought: Efficient llm reasoning with adaptive cognitive-inspired sketching. In *Proceedings of the 2025 Conference on Empirical Methods in Natural Language Processing*, pages 24307–24331, 2025.
- [3] Tianle Cai, Yuhong Li, Zhengyang Geng, Hongwu Peng, Jason D Lee, Deming Chen, and Tri Dao. Medusa: Simple llm inference acceleration framework with multiple decoding heads. *arXiv preprint arXiv:2401.10774*, 2024.
- [4] Sicheng Feng, Gongfan Fang, Xinyin Ma, and Xinchao Wang. Efficient reasoning models: A survey. *arXiv preprint arXiv:2504.10903*, 2025.
- [5] Fabian Gloeckle, Badr Youbi Idrissi, Baptiste Rozière, David Lopez-Paz, and Gabriel Synnaeve. Better & faster large language models via multi-token prediction. *arXiv preprint arXiv:2404.19737*, 2024.
- [6] Daya Guo, Dejian Yang, Haowei Zhang, Junxiao Song, Peiyi Wang, Qihao Zhu, Runxin Xu, Ruoyu Zhang, Shirong Ma, Xiao Bi, et al. Deepseek-r1: Incentivizing reasoning capability in llms via reinforcement learning. *arXiv preprint arXiv:2501.12948*, 2025.
- [7] Tingxu Han, Zhenting Wang, Chunrong Fang, Shiyu Zhao, Shiqing Ma, and Zhenyu Chen. Token-budget-aware llm reasoning. In *Findings of the Association for Computational Linguistics: ACL 2025*, pages 24842–24855, 2025.
- [8] Shibo Hao, Sainbayar Sukhbaatar, DiJia Su, Xian Li, Zhiting Hu, Jason Weston, and Yuandong Tian. Training large language models to reason in a continuous latent space. *arXiv preprint arXiv:2412.06769*, 2024.
- [9] Aaron Jaech, Adam Kalai, Adam Lerer, Adam Richardson, Ahmed El-Kishky, Aiden Low, Alec Helyar, Aleksander Madry, Alex Beutel, Alex Carney, et al. Openai o1 system card. *arXiv preprint arXiv:2412.16720*, 2024.
- [10] Yuhui Li, Fangyun Wei, Chao Zhang, and Hongyang Zhang. Eagle-3: Scaling up inference acceleration of large language models via training-time test. *arXiv preprint arXiv:2503.01840*, 2025.
- [11] Haotian Luo, Li Shen, Haiying He, Yibo Wang, Shiwei Liu, Wei Li, Naiqiang Tan, Xiaochun Cao, and Dacheng Tao. O1-pruner: Length-harmonizing fine-tuning for o1-like reasoning pruning. *arXiv preprint arXiv:2501.12570*, 2025.
- [12] Bo Lv, Yasheng Sun, Junjie Wang, and Haoxiang Shi. Onelaten: Single-token compression for visual latent reasoning. *arXiv preprint arXiv:2602.13738*, 2026.

- [13] Mohammad Samragh, Arnav Kundu, David Harrison, Kumari Nishu, Devang Naik, Minsik Cho, and Mehrdad Farajtabar. Your llm knows the future: Uncovering its multi-token prediction potential. *arXiv preprint arXiv:2507.11851*, 2025.
- [14] Xuan Shen, Yizhou Wang, Xiangxi Shi, Yanzhi Wang, Pu Zhao, and Jiuxiang Gu. Efficient reasoning with hidden thinking. *arXiv preprint arXiv:2501.19201*, 2025.
- [15] Zhenyi Shen, Hanqi Yan, Linhai Zhang, Zhanghao Hu, Yali Du, and Yulan He. Codi: Compressing chain-of-thought into continuous space via self-distillation. *arXiv preprint arXiv:2502.21074*, 2025.
- [16] Yang Sui, Yu-Neng Chuang, Guanchu Wang, Jiamu Zhang, Tianyi Zhang, Jiayi Yuan, Hongyi Liu, Andrew Wen, Shaochen Zhong, Na Zou, et al. Stop overthinking: A survey on efficient reasoning for large language models. *arXiv preprint arXiv:2503.16419*, 2025.
- [17] Wenhui Tan, Jiaze Li, Jianzhong Ju, Zhenbo Luo, Ruihua Song, and Jian Luan. Think silently, think fast: Dynamic latent compression of llm reasoning chains. *arXiv preprint arXiv:2505.16552*, 2025.
- [18] Kimi Team, Angang Du, Bofei Gao, Bowei Xing, Changjiu Jiang, Cheng Chen, Cheng Li, Chenjun Xiao, Chenzhuang Du, Chonghua Liao, et al. Kimi k1. 5: Scaling reinforcement learning with llms. *arXiv preprint arXiv:2501.12599*, 2025.
- [19] Yifan Wang, Shiyu Li, Peiming Li, Xiaochen Yang, Yang Tang, and Zheng Wei. Render-of-thought: Rendering textual chain-of-thought as images for visual latent reasoning. *arXiv preprint arXiv:2601.14750*, 2026.
- [20] Jason Wei, Xuezhi Wang, Dale Schuurmans, Maarten Bosma, Fei Xia, Ed Chi, Quoc V Le, Denny Zhou, et al. Chain-of-thought prompting elicits reasoning in large language models. *Advances in neural information processing systems*, 35:24824–24837, 2022.
- [21] Heming Xia, Chak Tou Leong, Wenjie Wang, Yongqi Li, and Wenjie Li. Tokenskip: Controllable chain-of-thought compression in llms. *arXiv preprint arXiv:2502.12067*, 2025.
- [22] Violet Xiang, Charlie Snell, Kanishk Gandhi, Alon Albalak, Anikait Singh, Chase Blagden, Duy Phung, Rafael Rafailov, Nathan Lile, Dakota Mahan, et al. Towards system 2 reasoning in llms: Learning how to think with meta chain-of-thought. *arXiv preprint arXiv:2501.04682*, 2025.
- [23] Silei Xu, Wenhao Xie, Lingxiao Zhao, and Pengcheng He. Chain of draft: Thinking faster by writing less. *arXiv preprint arXiv:2502.18600*, 2025.
- [24] Chenxu Yang, Qingyi Si, Yongjie Duan, Zheliang Zhu, Chenyu Zhu, Qiaowei Li, Minghui Chen, Zheng Lin, and Weiping Wang. Dynamic early exit in reasoning models. *arXiv preprint arXiv:2504.15895*, 2025.
- [25] Jintian Zhang, Yuqi Zhu, Mengshu Sun, Yujie Luo, Shuofei Qiao, Lun Du, Da Zheng, Huajun Chen, and Ningyu Zhang. Lightthinker: Thinking step-by-step compression. In *Proceedings of the 2025 Conference on Empirical Methods in Natural Language Processing*, pages 13318–13339, 2025.

## A Inference Efficiency Analysis

To evaluate practical efficiency, we compare the average wall-clock inference time of SLT against the explicit SFT-CoT baseline across four benchmarks (Figure 6). SLT consistently accelerates inference on both backbones, but the speedup is notably more pronounced on Qwen3-4B. This discrepancy stems from the relative scale of the auxiliary modules. Our framework introduces a lightweight 1-layer feature decoder and a 2-layer compressor, which incur a similar, marginal absolute overhead on both models. However, because Qwen3-4B is significantly larger than Llama-3.2-1B, bypassing its heavy autoregressive generation yields much greater relative computational savings.

Furthermore, we observe that the relative speedup on GSM-Hard is smaller compared to SVAMP or MultiArith. This aligns perfectly with our observations in Section 4.2: GSM-Hard contains extensive, precision-critical numerical reasoning where forced compression is unsafe. Consequently, our dynamic gating mechanism safely falls back to explicit CoT to preserve downstream accuracy. This deliberate trade-off naturally requires more explicit tokens, explaining the comparatively higher inference time on this specific dataset while avoiding the severe performance degradation seen in aggressive baseline methods.

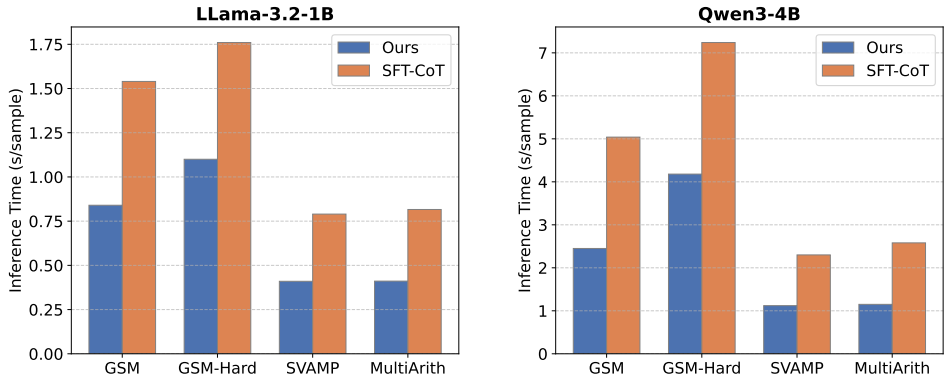


Figure 6: Average inference time comparison. Inference times for all models are measured on the GSM8k-AugNL dataset using a single A6000 GPU. SLT achieves substantial wall-clock speedups, particularly on the larger Qwen3-4B backbone, while dynamically adjusting computational effort on harder datasets like GSM-Hard.

## B Inference Dynamics: Surpassing Explicit CoT via Threshold Modulation

Complementing the main results in Section 4.2, we explore whether inference-time threshold modulation can actively surpass the original SFT-CoT baseline. We trace the performance-efficiency Pareto frontier by varying the gating logit bias  $\gamma \in [-1.0, 1.0]$ . As illustrated in Figure 7, setting a conservative threshold ( $\gamma > 0$ ) yields remarkable gains. Specifically, as  $\gamma$  approaches +1.0, SLT actively outperforms the SFT-CoT baseline on critical benchmarks like GSM and GSM-Hard, while maintaining a substantially shorter token length. This indicates that selective compression acts as an implicit denoiser: by safely compressing linguistic fluff while explicitly preserving mathematical pivots, it mitigates the cascading hallucination errors typical of overly verbose explicit chains.

Conversely, corroborating our theoretical intuition in Section 3.3, pushing the framework into aggressive compression ( $\gamma < 0$ ) reveals a stark cliff of diminishing marginal returns. As the threshold drops below zero, the horizontal gaps between points narrow significantly—indicating a physical limit to further length reduction—while accuracy drops precipitously. This confirms that forcing latent transitions beyond the model’s intrinsic epistemic confidence aggressively destroys the underlying mathematical logic. Ultimately, this dynamic controllability allows practitioners to adopt a moderately conservative threshold ( $\gamma \in [0.4, 1.0]$ ), unlocking an optimal operating regime that eclipses the explicit baseline’s accuracy while consistently reducing computational cost.

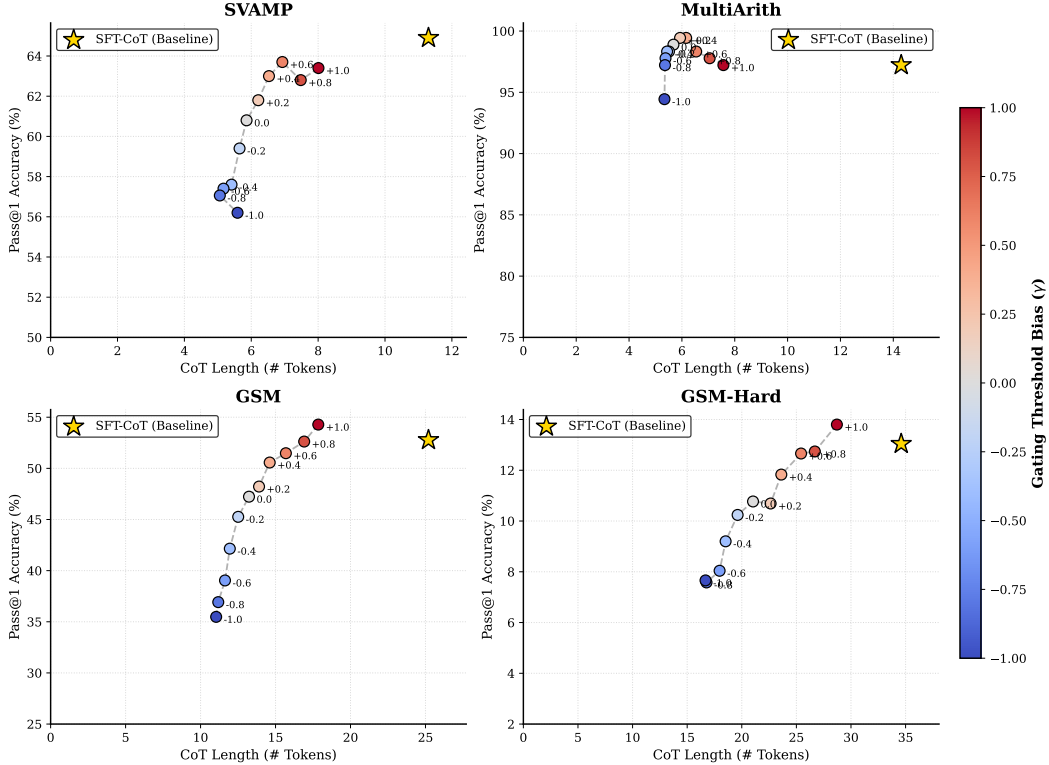


Figure 7: Accuracy-efficiency Pareto frontier across different test datasets. By modulating the gating threshold bias  $\gamma \in [-1.0, 1.0]$ , SLT traces a smooth efficiency-accuracy trade-off. The gold star represents the SFT-CoT baseline. Notably, under conservative thresholds ( $\gamma > 0$ , red points), SLT frequently surpasses the explicit CoT accuracy ceiling while maintaining lower computational costs. Conversely, aggressive compression ( $\gamma < 0$ , blue points) exhibits diminishing marginal returns on length reduction and severe accuracy drops.

## C Implementation Details

To ensure reproducibility, the core architectural specifications and hyperparameter configurations across all training stages are summarized in Table 6. We evaluate our framework on two prominent base models: **Llama-3.2-1B** and **Qwen3-4B**.

**Architecture & Stage 1.** The latent compressor  $\mathcal{C}$  is built with 2 cross-attention layers, while the feature decoder  $\mathcal{D}$  uses a single transformer block. To build the representation foundation smoothly, Stage 1 employs a two-phase warmup strategy: we first freeze the primary LLM and train only the compressor for 5 epochs. Subsequently, we inject LoRA adapters ( $r = 128$ ,  $\alpha = 32$ ) into the LLM and jointly train for another 5 epochs.

**Stage 2 & Stage 3.** In the Stage 2 local dynamics alignment, we set the feature decoder’s look-ahead window to  $K = 4$ . Combined with the primary LLM’s initial token, this creates a maximum latent span of 5 tokens, aligning perfectly with the capacity limits discussed in Appendix E. The loss components are balanced with a 1 : 2 ratio, placing heavier emphasis on the gating module ( $\mathcal{L}_{\text{gate}}$ ) to strictly penalize boundary errors. Finally, during the Stage 3 GRPO phase, we sample 8 distinct trajectories per prompt. The delayed reward strongly enforces exact factual correctness ( $\alpha = 1.0$ ) while applying a conservative penalty for explicit token generation ( $\beta = 0.01$  per token), ensuring the policy prioritizes logical rigor over reckless compression.

Table 6: Key hyperparameters and architectural configurations for the three-stage training pipeline. Note that the primary LLM is strictly frozen during Stage 2. For the Stage 3 RL optimization, Llama-3.2-1B undergoes full-parameter tuning, whereas Qwen3-4B is optimized via LoRA due to computational resource constraints.

Stage	Hyperparameter	Value
Stage 1	Phase 1 Training (Frozen LLM)	5 Epochs
	Phase 2 Training (LoRA tuning)	5 Epochs
	LoRA Configuration	$r = 128, \alpha = 32$
	Learning Rate	$1 \times 10^{-4}$
Stage 2	Look-ahead Window ( $K$ )	4
	Training (Frozen LLM)	3 Epochs
	Loss Weight ( $\mathcal{L}_{\text{vocab}} : \mathcal{L}_{\text{gate}}$ )	1 : 2
	Learning Rate	$1 \times 10^{-4}$
Stage 3	GRPO Group Size	8
	Correctness Reward ( $\alpha$ )	1.0
	Token Penalty ( $\beta$ )	0.01

## D Interpretability and Visualization of Compression Trajectories

**Visualization of Compression Trajectories.** To intuitively demonstrate the Selective Latent Thinking (SLT) mechanism, Figure 8 visualizes the actual generation trajectories. The directed arrows represent the autoregressive forward pass. Green nodes represent instances where multiple explicit tokens are functionally compressed into a single continuous latent vector ( $\mathbf{z}_{\text{comp}}$ ), while blue nodes indicate explicit tokens preserved by the confidence gate.

Across both natural language (Case 1) and structured equation (Case 2) formats, the model exhibits a clear "semantic routing" behavior. Predictable linguistic connective tissues (e.g., ["She", "needs", " "]) and deterministic operational transitions (e.g., ["20", "\*"]) are consistently absorbed into compact latent blocks. Conversely, immediately prior to generating high-entropy mathematical pivots—such as exact intermediate values (1, 300) or final answers (24, 650)—the gate aggressively halts compression. This forces the LLM to articulate fragile numerical entities explicitly. Crucially, the continuous autoregressive flow (blue arrows) confirms this is not extractive token skipping: the latent green nodes successfully carry the full semantic and causal payload required to accurately condition the subsequent explicit blue tokens.

## E Ablation on Maximum Compression Boundary

To unpack the truncation effect observed in Section 4.2, we ablate the maximum look-ahead boundary  $c_{\text{max}}$  on the GSM benchmark using the Ours-SFT setting (Table 7). The results reveal a strict capacity limit for single-vector continuous representations. Pushing the boundary to  $c_{\text{max}} \geq 6$  causes a precipitous accuracy drop (down to 33.53%). This highlights a severe **representation bottleneck**: forcing a single latent vector to simulate overly long discrete trajectories inevitably induces compounding uncertainty and destroys mathematical fidelity. Conversely, over-constraining the window ( $c_{\text{max}} = 3$ ) artificially fragments natural linguistic phrases, degrading both efficiency and accuracy due to suboptimal semantic chunking. Ultimately, the optimal manifold lies at  $c_{\text{max}} \in [4, 5]$  (peaking at 45.03%), which perfectly scales to absorb predictable linguistic transitions while safely halting before critical high-entropy numerical pivots.

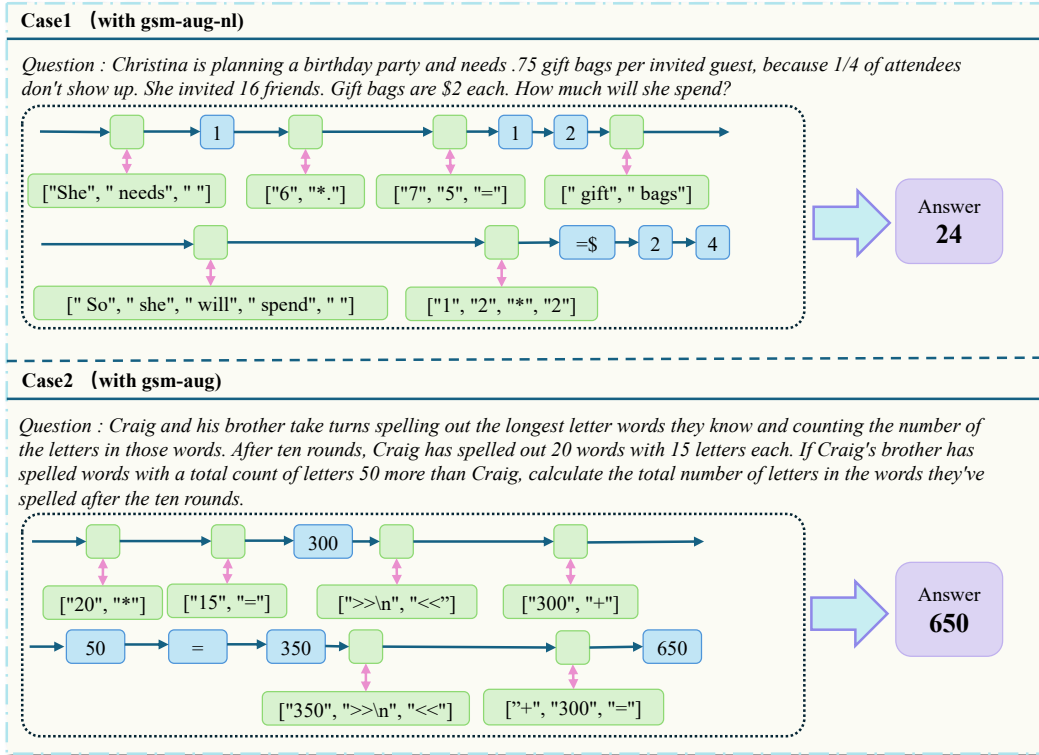


Figure 8: Visualization of SLT generation trajectories. The timeline arrows illustrate the causal autoregressive flow. Green nodes represent compressed continuous latent vectors ( $\mathbf{z}_{\text{comp}}$ ) replacing the bracketed explicit strings below them. Blue nodes are explicit tokens triggered by the confidence gate’s fallback mechanism, ensuring strict accuracy for numerical pivots.

Table 7: Impact of varying the maximum compression boundary ( $c_{\text{max}}$ ) on GSM performance. Pushing  $c_{\text{max}} \geq 6$  degrades reasoning accuracy, revealing the intrinsic capacity limit of continuous representations.

Maximum Boundary ( $c_{\text{max}}$ )	Pass@1 Accuracy (%)	Explicit CoT Length (#L)
7	33.53	12.50
6	36.09	12.43
5 (Default)	42.46	13.42
4	<b>45.03</b>	14.78
3	44.20	15.59